Laser cooling, trapping and spectroscopy of calcium isotopes

Mollema, Albert Kornelis

Chapter 2

Theory

In this chapter, the theoretical aspects needed to describe the optical decelerating and cooling processes used in the Al^{41}Catraz setup are provided, as well as a brief description of the structure of the calcium atom.

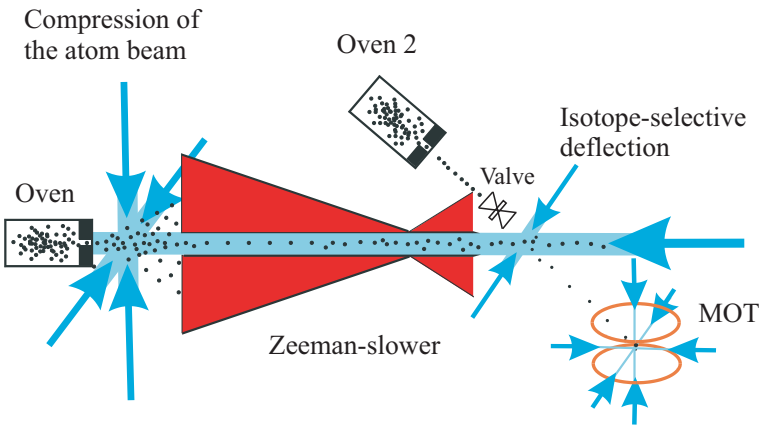

Figure 2.1: *Schematic overview of our Al^{41}Catraz setup for separation and detection of Ca isotopes.*

The essential role played by optical techniques is obvious from fig. 2.1, which shows a schematic picture of the setup. In summary, the setup works as follows. Atoms are evaporated from the oven and are entering the Zeeman slower. Here, by means of a counter propagating laser, atoms of velocities up to approximately 1000 m/s can be decelerated to $\sim 50-100$ m/s. After the Zeeman slower, the atoms proceed towards the optical deflection stage. At this point, the desired isotopes are deflected over an angle of 30° towards the Magneto Optical Trap (MOT). In this MOT, atoms are trapped and

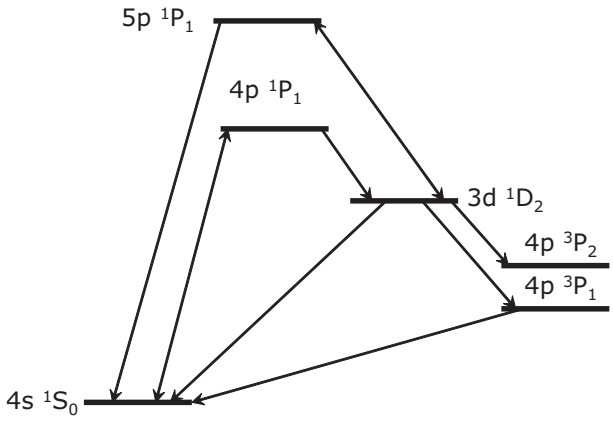

Figure 2.2: *The most relevant $4snl$ energy levels of the calcium atom.*

detected by measuring their fluorescence.

2.1 The electronic structure of the calcium atom

In our experiment, the $4s^2\ ^1S_0$ - $4s4p\ ^1P_1$ transition is used for cooling (see fig. 2.2). In this section, some general aspects of the electronic structure of calcium are discussed, together with the most important features of the calcium atom that play a role in the experiments that we describe.

For most practical purposes, alkaline earth atoms can be considered as two-electron atoms with an inert electronic core. For Ca the relevant ground electronic configuration is $4s^2$. In a two electron system, the spins $\vec{s}_1$ and $\vec{s}_2$ and the orbital momenta $\vec{l}_1$ and $\vec{l}_2$ determine the total spin $\vec{S}$ and orbital momentum $\vec{L}$ respectively. The coupling of these quantities is governed by the rules of LS or Russel-Saunders coupling [36]. The total orbital momentum $\vec{L}$ gives rise to a magnetic field $\vec{B}_L$ and the total spin $\vec{S}$ has a magnetic moment $\vec{\mu}_S$ associated to it which aligns itself in the magnetic field. The interaction between these two results in coupling of the two angular momenta $\vec{L}$ and $\vec{S}$ to the total angular momentum $\vec{J}$

$$\vec{J} = \vec{L} + \vec{S}. \tag{2.1}$$

An important quantum number is the magnetic quantum number m_J. It describes the magnitude of the z-component of $\vec{J}$

$$|\vec{J}|_z = m_J\hbar, \quad m_J = J, J-1, \ldots, -J \tag{2.2}$$

If a weak external magnetic field $\vec{B}_0$ with magnitude B_0 is applied, the states with different values of m_J will split into a Zeeman multiplet. The energy difference between adjacent components is given by

$$\Delta E_{m_J,m_{J-1}} = g_J \mu_B B_0, \tag{2.3}$$

since the absolute shift is $g_J m_J \mu_B B_0$ with μ_B the Bohr magneton, $\mu_B = 13.9962458 \cdot 10^9$ Hz/T [37]. The values for g_J can be calculated with

$$g_J = 1 + \frac{J(J+1) + S(S+1) - L(L+1)}{2J(J+1)}. \tag{2.4}$$

In the case of singlet terms such as $^1S_0$ and $^1P_1$ $S = 0$ implying $L = J$ and $g_J = 1$. The resulting energy shifts are indicated in Fig. 2.3.

2.1.1 Hyperfine structure

For atoms which have a nuclear spin, the total angular momentum of the electrons $\vec{J}$ and the nuclear spin $\vec{I}$ couple to a new total angular momentum $\vec{F}$ [36]

$$\vec{F} = \vec{J} + \vec{I}. \tag{2.5}$$

The magnitude of the z component of $\vec{F}$ is given as

$$|\vec{F}|_z = m_F \hbar \text{ with } m_F = F, F-1, \ldots, -F. \tag{2.6}$$

In a weak external magnetic field $\vec{B}_0$ with magnitude B_0 the shift of the hyperfine components is given by

$$\Delta E_{HFS} = g_F \mu_B B_0 m_F \tag{2.7}$$

with

$$g_F = g_J \frac{F(F+1) + J(J+1) - I(I+1)}{2F(F+1)} - g_I \frac{\mu_N}{\mu_B} \frac{F(F+1) + I(I+1) - J(J+1)}{2F(F+1)} \tag{2.8}$$

where μ_N is the nuclear magneton and $\mu_N/\mu_B \cong 1/1836$ and g_I the nuclear g-factor which has the value -0.456 for ^{41}Ca and -0.376 for ^{43}Ca [37]. The explicit g_F values

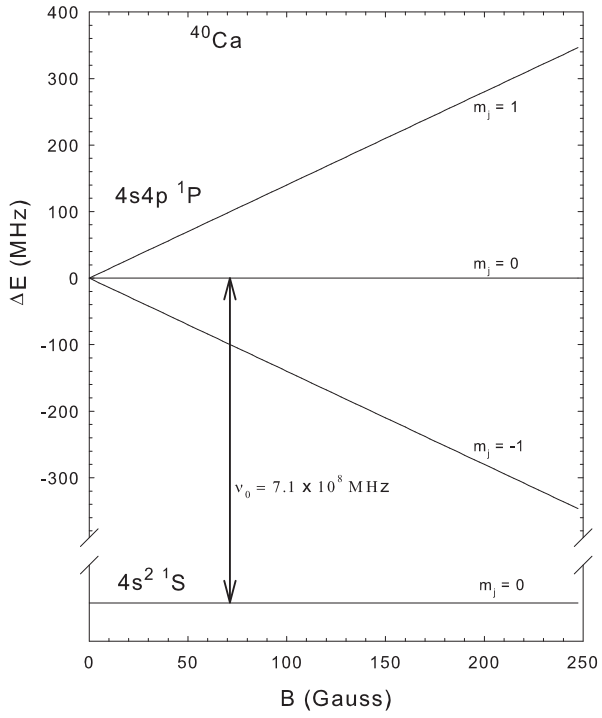

Figure 2.3: *Zeeman shift of the* $^{40}Ca\ 4s4p\,^1P_1$ *state as a function of magnetic field.*

for the relevant levels in ^{41}Ca and ^{43}Ca are given in Table 2.1. Eq. (2.8) holds for magnetic field strengths as produced within a few mm around the centre of the MOT. For strong B-fields, I and J decouple and the situation can then be described by

$$\Delta E_{HFS} = g_J \mu_B m_J B_0 + A m_I m_J - g_I \mu_N m_I B_0 \tag{2.9}$$

where A is the hyperfine structure constant which is negative since the nuclear magnetic moments of ^{41}Ca and ^{43}Ca are negative. There is no analytical expression connecting these two situations, so for calculating hyperfine splittings for a long range of the B-field, one has to rely on numerical methods [38]. Results of such a numerical code [20] are shown in Fig. 2.4. Because the nuclear magnetic moments are negative the sequence of hyperfine levels is inverted, i.e., $F = 9/2$ is the most strongly bound one. In addition, for weak fields, the sequence of the m_F states of the $F = 5/2$ level is inverted ($g_{F=5/2} < 0$, see Table 2.1). For $F = 7/2$, g_F is very small so the splitting within the $F = 7/2$ level is very weak.

In the absence of external fields, the frequency shift with respect to the ^{40}Ca transition of any hyperfine level of the odd isotopes is given by

$$\Delta\nu_F = \Delta\nu_{IS} + \frac{A}{2}C + \frac{B}{4}\frac{\frac{3}{2}C(C+1) - 2I(I+1)J(J+1)}{(2I-1)(2J-1)IJ} \tag{2.10}$$

where $\Delta\nu_{IS}$ is the "centre of gravity" (cg) value of the isotope shift and C is defined as $C = F(F+1) - I(I+1) - J(J+1)$. Using the values of A and B and $\Delta\nu_{IS}$ that were experimentally determined by Nörtershäuser et al. [39] (see Table 2.2) leads to the following isotope shifts (in MHz) for the $4s^2\ ^1S_0$ - $4s4p\ ^1P_1$ transition [20] in ^{41}Ca

$$\begin{aligned} \Delta\nu_{9/2} &= 154 \\ \Delta\nu_{7/2} &= 248 \\ \Delta\nu_{5/2} &= 303 \end{aligned} \tag{2.11}$$

and for ^{43}Ca

$$\begin{aligned} \Delta\nu_{9/2} &= 554 \\ \Delta\nu_{7/2} &= 633 \\ \Delta\nu_{5/2} &= 675 \end{aligned} \tag{2.12}$$

2.1.2 Dipole transitions

In the case of odd isotopes, the hyperfine interaction complicates the electronic structure and therefore the optical transitions between the $4s^2\ ^1S_0$ and $4s4p\ ^1P_1$ levels. Following the argument of Ref. [40], the relative transition strengths can be calculated

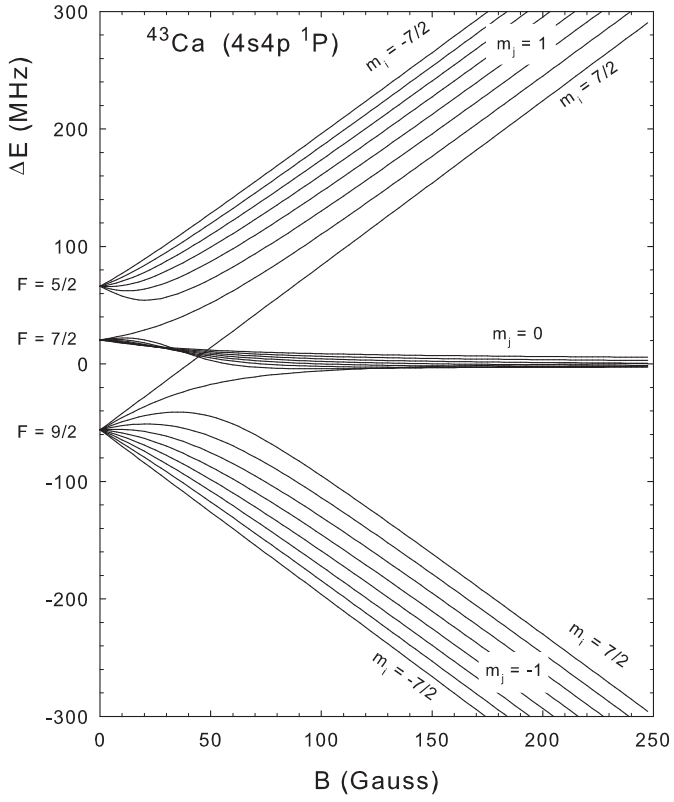

(a)

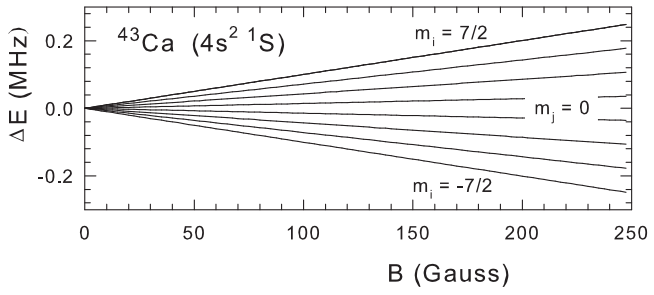

(b)

Figure 2.4: *The hyperfine splitting in the ^{43}Ca $4s4p\,^1P_1$ state (a) and the $4s4s\,^1S_0$ ground state (b) as a function of the magnetic field.*

Isotope, L	$F = 5/2$	$F = 7/2$	$F = 9/2$
^{43}Ca, $L = 1$	-0.286	0.0637	0.222
^{41}Ca, $L = 1$	-0.285	0.0637	0.222
^{43}Ca, $L = 0$		2.05×10^{-4}	
^{41}Ca, $L = 0$		2.48×10^{-4}	

Table 2.1: *Calculated g_F values of the hyperfine levels of the singlet terms of the cooling transition using Eq. 2.8.*

Isotope	$\Delta\nu_{IS}$ *(cg)*	*A*	*B*
^{41}Ca	221.8(8)	$-18.58(13)$	$-5.1(11)$
^{43}Ca	611.8(3)	$-15.54(3)$	$-3.48(13)$

Table 2.2: *$\Delta\nu_{IS}$ (cg), A and B values obtained by [39]. All values in are given in MHz.*

using the appropriate relative linestrength coefficients C_i, which for the even isotopes are given by

$$C_i = (-1)^{L'+S-m'_J}\sqrt{(2J+1)(2J'+1)} \times \left\{ \begin{array}{ccc} L' & J' & S \\ J & L & 1 \end{array} \right\} \times \left(\begin{array}{ccc} J & 1 & J' \\ m_J & q & -m'_J \end{array} \right) \tag{2.13}$$

where S is the spin quantum number,() and {} are Wigner 3j and 6j symbols, respectively. The quantum numbers with a prime are quantum numbers of the excited state, the others of the ground state. The polarization of the light is indicated by q: $q = +1$ for σ^+ polarized light, $q = 0$ for linear polarized light and $q = -1$ for σ^- polarized light. For our simple $^1S_0$ - $^1P_1$ transition using σ^+ light ($m_j = 0$ - $m'_j = 1$, obeying $m_j + q - m'_j = 0$) the angular part of the transition matrix element is [20]

$$(-1)^{(0)} \cdot \sqrt{3} \cdot \sqrt{1/3} \cdot \sqrt{1/3} = \frac{1}{3}\sqrt{3}$$

For the odd isotopes one has to include the nuclear spin, and the expression becomes

$$C_i = (-1)^{1+L'+S+J+J'+I-m'_F}\sqrt{(2J+1)(2J'+1)(2F+1)(2F'+1)} \times \left\{ \begin{array}{ccc} L' & J' & S \\ J & L & 1 \end{array} \right\} \left\{ \begin{array}{ccc} J' & F' & I \\ F & J & 1 \end{array} \right\} \left(\begin{array}{ccc} F & 1 & F' \\ m_F & q & -m'_F \end{array} \right) \tag{2.14}$$

In Figure 2.5 the calculated relative transition strengths are shown. They are multiplied by a factor of 252 to have all integer numbers. This scheme is the same for ^{41}Ca, ^{43}Ca, ^{45}Ca and ^{47}Ca, because they have the same nuclear spin. Important to note is that the

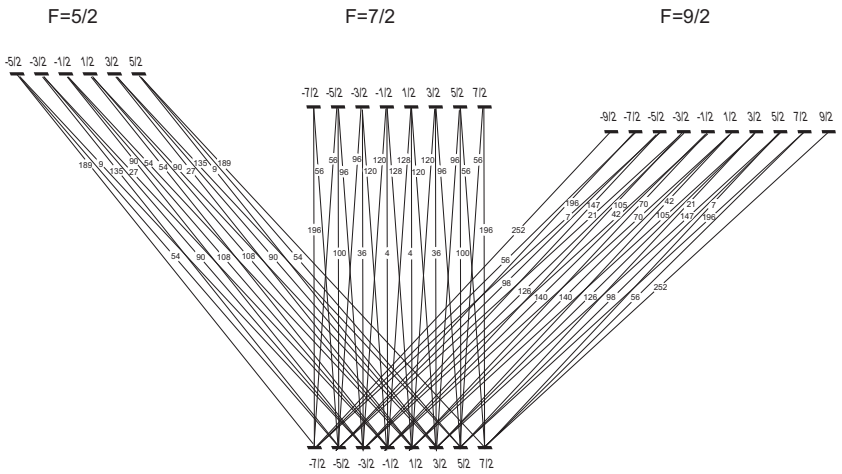

Figure 2.5: *The transition strengths between the excited state $^1P_1$ and the ground state $^1S_0$ for Ca-41, 43, 45 and 47. The strength is given in the smallest possible integer numbers. Adapted from [20, 38].*

angular part of the transition matrix element for a transition in any of the odd isotopes from $m_F = 7/2$ to $m'_F = 9/2$ is [20]

$$(-1)^{(4)} \cdot \sqrt{240} \cdot \sqrt{1/3} \cdot -1/2\sqrt{1/6} \cdot -\sqrt{1/10} = \frac{1}{3}\sqrt{3}$$

and thus equal in strength to the transition in the even isotopes. This is important for the isotope selectivity that can be reached in the experiment. The sum of the transition strengths for the $9/2$, $7/2$ and $5/2$ states varies with $(2F+1)$. The ratio between the total transition strengths therefore is $10:8:6$.

For (optical) dipole transitions the following selection rules apply: $\Delta J = 0, \pm 1$ (but not $J = 0 - J' = 0$), $\Delta m_J = 0, \pm 1$, $\Delta F = 0, \pm 1$, $\Delta m_F = 0, \pm 1$, $\Delta l = \pm 1$, $\Delta L = 0, \pm 1$, $\Delta S = 0$

2.1.3 Nuclear spin

The nuclear spin of the odd isotopes of calcium (see table 2.3) can be understood from the Nuclear Shell Model (NSM). In this model, we may assume that each nucleon occupies a well-defined energy level [41]. The existence of these discrete energy levels for the nucleons in the nucleus is reminiscent of the atomic electron cloud. In the nucleus the nucleons move inside a potential produced by the other nucleons. In both cases discrete energy levels, or shells, arise which are filled according to the constraints of the Pauli principle. The energy levels can be calculated for both protons and neutrons. If for a certain nucleus both the neutron and the proton shell is filled, i.e. both shells are closed, the nucleus is exceptionally stable. These nuclei are called doubly magic.

Isotope	*Rel. nat. abundance*	*Nucl. spin*	*Half-life*	*Isotope-shift (MHz)*
39	-	3/2	859.6 ms	
40	0.9694	0	stable	0
41	$1 \cdot 10^{-14}$	7/2	103,000 yrs	154/248/303
42	0.0065	0	stable	393
43	0.0014	7/2	stable	554/633/675
44	0.0209	0	stable	774
45	-	7/2	162.61 d	
46	0.00004	0	stable	1160
47	-	7/2	4.536 d	
48	0.0019	0	$6 \cdot 10^{18}$ yrs	1513
49	-	3/2	8.718 m	

Table 2.3: *Properties of the calcium isotopes. Shown are the relative natural abundance, the nuclear spin, the half-life time and for the stable isotopes the isotope shift of the cooling transition relative to ^{40}Ca in MHz. The shifts given for ^{41}Ca and ^{43}Ca are for the 9/2, 7/2 and 5/2 hyperfine components.*

Calcium in this sense turns out to be a rather remarkable element: two of its isotopes are doubly magic: ^{40}Ca and ^{48}Ca. ^{40}Ca closes the $1d_{(3/2)}$ shell while ^{48}Ca closes the neutron $1f_{7/2}$ shell.

In closed-shell nuclei the total angular momentum couples to 0 so for ^{40}Ca we have $I^P = 0^+$. The valence shell for ^{40}Ca is $f_{7/2}$, therefore ^{41}Ca has $I^P = \frac{7}{2}^-$ Adding more neutrons the residual attractive nuclear force and the Pauli principle combines to pair neutrons with opposite spin so that all odd Ca isotopes ($A = 41$ through 47) have spin $\frac{7}{2}^-$. The spin of ^{39}Ca can be understood as a hole in the closed $d_{(3/2)}$ shell and thus has the value $I^P = \frac{3}{2}^+$.

2.1.4 Isotope shift

The isotope shift $(\Delta\nu_{IS})_i^{AA'}$ of a particular optical transition i of an isotope with mass number A' relative to the isotope with mass number A is the sum of a shift $\Delta\nu_{mass}$ due to change of mass of the nucleus and of a shift resulting from the variation of the nuclear charge radius $\delta\langle r^2\rangle^{AA'}$. It can be written as [39]

$$(\Delta\nu_{IS})_i^{AA'} = M_i \frac{A' - A}{AA'} + F_i \delta\langle r^2\rangle^{AA'},$$

where M_i is the mass-shift coefficient and F_i the field-shift coefficient. The measured isotope shifts for the relevant calcium isotopes as determined in [39] are given in table 2.3.

2.2 Deceleration of neutral atoms

Consider an atom that moves in a certain direction, and a counter-propagating laser beam with a frequency just below the atomic resonance. For specific atomic velocities the Doppler shift due to the velocity of the atom will shift the laser light in resonance with the atomic transition. The atom will be excited to an excited state. When the atom decays to its ground state again, it will emit a photon. In principle, there is no preferred direction into which this photon will be emitted. The laser photons on the other hand are propagating in a fixed direction. This results in a situation where there is on average no net momentum change due to the spontaneous emission of photons, but only due to the absorption of laser photons by the atom. Because of this, the atom's velocity component anti-parallel to the propagation direction of the laser beam will be reduced.

The decelerating optical force on atoms is thus caused by the momentum transfer resulting from the absorption of light by the atom. The photon carries energy ($E = \hbar\omega$), angular momentum ($L = \hbar$) and momentum ($p = \hbar k$). In these equations ω is the frequency of the light, $\hbar$ the Planck constant divided by 2π and k the norm of the wave vector $\vec{k}$. When an atom absorbs a photon, it stores energy by going to an excited state, and changes momentum by an amount equal to the photon recoil of $\hbar k$. When the atom decays to its ground state, it releases energy by emitting a photon, and as mentioned before the associated recoil momenta average out over many excitation-decay cycles. To achieve maximal deceleration of the atom, one has to make a careful choice of the laser light frequency. Tuning the frequency of the laser light below (to the red of) the atomic resonance makes it more likely that atoms absorb light from the laser beam that is propagating opposite to their own motion.

We consider a two level atom with a frequency difference ω_0 between ground and excited state, and a laser beam that we assume to be a plane wave of frequency ω_l and wavelength λ. The detuning of the laser frequency from the atomic resonance frequency is given by $\delta = \omega_l - \omega_0$. The Doppler shift as seen by an atom moving with a velocity v opposite to the propagation direction of the laser beam is given by $\vec{k} \cdot \vec{v}$, which results in a total detuning of $\delta - \vec{k} \cdot \vec{v}$. The excited-state population decays radiatively to the ground state at a rate Γ. The strength of the laser induced coupling between the ground and excited state is characterized by a saturation intensity I_s such that when the laser intensity $I = I_s$ the transition is power broadened by a factor of $\sqrt{2}$ [16]. This saturation intensity is related to the Rabi frequency Ω by the on-resonance saturation parameter $s_0 \equiv I/I_s = 2\Omega^2/\Gamma^2$, and is also given as $I_s = \pi hc/3\lambda^3\tau$, with h Planck's constant, c the speed of light and τ the natural lifetime of the excited state [40, 42].

The radiation force exerted on atoms can be described as the momentum transfer $\Delta p = \hbar k$ times the total scattering rate $\Gamma_p = \Gamma\rho_{ee}$, where ρ_{ee} is the population of the excited state, which can be calculated from a solution of the optical Bloch equations (OBE):

$$\Gamma_p = \Gamma\rho_{ee} = \Gamma\frac{s_0/2}{1+s_0+(2\delta/\Gamma)^2}. \tag{2.15}$$

The force on the atoms can now be written as

$$\vec{F} = \hbar\vec{k}\Gamma_p. \tag{2.16}$$

At very high intensities ($s_0 \gg 1$), Γ_p saturates to $\Gamma/2$, resulting in $\vec{F}_{max} = \hbar\vec{k}\Gamma/2$. Taking the Doppler shift into account, the light force on the atoms is given by

$$\vec{F} = \hbar\vec{k}\frac{\Gamma}{2}\frac{s_0}{1+s_0+[2(\delta-\vec{v}\cdot\vec{k})/\Gamma]^2}. \tag{2.17}$$

2.3 Optical molasses

In the case of a 1D optical molasses, we have two laser beams of the same frequency, but propagating in opposite direction. When the atom has a certain velocity it will see the light coming from the beams Doppler shifted. If the laser frequency is red detuned with respect to the resonance frequency, the light coming from the counter-propagating laser beam is closer to resonance than the frequency of the co-propagating laser beam. As a consequence, the probability that the atom will absorb light coming from the counter propagating laser beam is larger than the probability that it will absorb light from the other one, which means that the atom will be decelerated.

The force on the atoms in such an optical molasses configuration is easily calculated from Eq. (2.17) and found to be:

$$\vec{F}_{OM} = \hbar\vec{k}\frac{\Gamma}{2}\left[\frac{s_0}{1+s_0+[2(\delta-\vec{v}\cdot\vec{k})/\Gamma]^2} - \frac{s_0}{1+s_0+[2(\delta+\vec{v}\cdot\vec{k})/\Gamma]^2}\right]. \tag{2.18}$$

In the approximation that $|kv| \ll \Gamma$ and $|kv| \ll \delta$ one gets [16]:

$$\vec{F}_{OM} = 4\hbar\vec{k}s_0\frac{kv(2\delta/\Gamma)}{[1+(2\delta/\Gamma)^2]^2}. \tag{2.19}$$

The force is a damping force for all velocities if $\delta < 0$ and it is linear in v if $|kv| \ll |\delta|$ or $|kv| \ll \Gamma$, see fig. 2.6. If $\delta > 0$, the force accelerates the atoms. We can write the damping force as

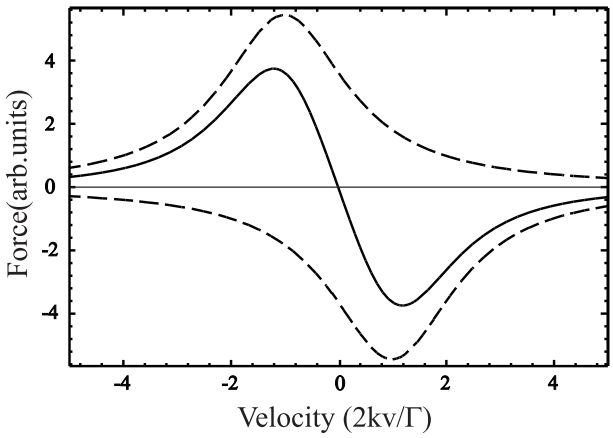

Figure 2.6: *The effective force (solid line) on the atoms in an optical molasses as a function of the velocity of the atom. The individual forces of the counter propagating laser beams are indicated by the dashed lines.*

$$\vec{F}_{OM} = -\beta\vec{v}, \tag{2.20}$$

with the damping coefficient

$$\beta = 4\hbar k^2 s_0 \frac{(2\delta/\Gamma)}{[1+(2\delta/\Gamma)^2]^2}. \tag{2.21}$$

The force F_{OM} has maxima near $v \approx \pm\Gamma\sqrt{s_0+1}/2k$ and decreases rapidly for larger velocities [15].

2.4 Doppler limit

The velocity of the atoms does not eventually go to zero. In 1979, Wineland and Itano [43] showed that the cooling of the atomic motion is limited by the heating resulting from the spontaneous emission of photons in random directions.

First we consider the damping force $\vec{F} = -\beta\vec{v}$. The rate at which the atom looses kinetic energy due to this force is given by [16]

$$\left(\frac{dE}{dt}\right)_{cool} = Fv = -\beta v^2. \tag{2.22}$$

The damping force reduces the average velocity of the atoms to zero, but while the mean velocity becomes zero, there is some continuous heating action by the laser beams that must be considered. An atom with almost zero velocity is as likely to absorb a photon from the beam travelling in the same direction as from the beam travelling in the opposite direction of the velocity of the atom. The absorption and the spontaneous emission that will follow can be modelled as a step of size $\hbar k$ in the random walk motion of the atom. Applying random walk theory (as described by the Fokker-Planck equation, see Ref. [40]) yields a diffusion coefficient [15]

$$D_0 = \frac{1}{2}\frac{d(p^2)}{dt} = 2\Gamma_p \hbar^2 k^2, \tag{2.23}$$

with p the momentum of the atom, which leads to a kinetic energy increase at a rate of

$$\left(\frac{dE}{dt}\right)_{heat} = \frac{\Gamma_p \hbar^2 k^2}{M} = \frac{D_0}{M}. \tag{2.24}$$

At equilibrium, the heating and cooling rates are equal, so $\left(\frac{dE}{dt}\right)_{heat} + \left(\frac{dE}{dt}\right)_{cool} = 0$. Since for a 1D problem we have $k_B T/2 = M v_{rms}^2/2$, this finally leads to a steady state temperature given by $k_B T = D_0/\beta$ [15,16] where k_B is the Boltzmann constant, which turns out to have a minimum at low laser intensities if $\delta = -\Gamma/2$ of

$$k_B T_{min} = \frac{\hbar\Gamma}{2}. \tag{2.25}$$

This minimum temperature is often referred to as the Doppler temperature, abbreviated as T_D. For calcium, this Doppler temperature is 831 μK. The model described above can be extended to 3 dimensions and to cases with higher laser intensities. Taking into account the detuning as well, one gets [16]:

$$k_B T_D = \frac{\hbar\Gamma}{4}\frac{1 + 6I/I_S + (2\delta/\Gamma)^2}{2|\delta|/\Gamma} \tag{2.26}$$

Examples of the results of this theory applied to Ca are shown in Fig. 2.7.

In 1988 Lett *et al.* [44] made careful measurements of the temperatures of optical molasses of sodium, and measured temperatures below the Doppler temperature, demonstrating that Doppler theory alone could not predict the temperature of atoms in an optical molasses accurately. In 1989 Dalibard and Cohen-Tannoudji [45] and Ungar *et al.* [46] presented theoretical models, that took into account the polarization gradients of the laser beams, that explained these measurements.

In contrast to the alkalines, measurements of the MOT cloud temperature of even alkaline-earth isotopes like ^{88}Sr (e.g. [17]) and ^{40}Ca (see [47–49] and also Chapter 6

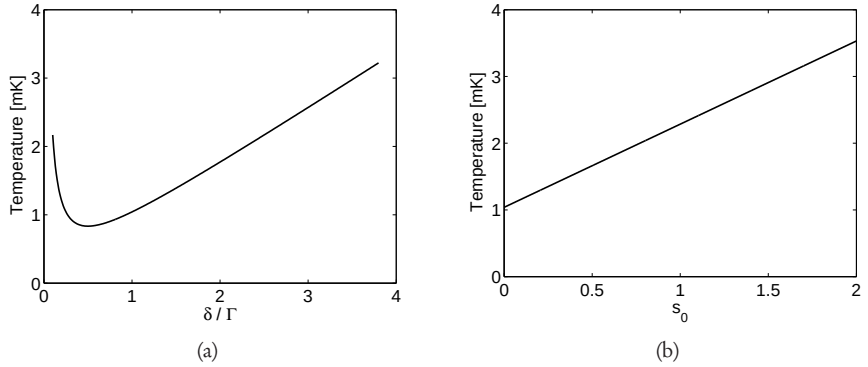

(a) (b)

Figure 2.7: *MOT temperatures calculated with Eq. 2.26. (a) Temperature vs. relative detuning δ/Γ in low laser intensity approximation. (b) Temperature vs. relative intensity $s_0 = I/I_S$ with $|\delta/\Gamma| = 1$.*

of this thesis) yielded temperatures that are systematically higher than predicted by Doppler theory. Only very recently possible explanations for these results have been proposed [50, 51] (see Chapter 6 for a discussion).

2.5 Applications

2.5.1 The Zeeman slower

In the first section of this chapter, we saw that in principle it is possible to slow down neutral atoms with laser light. The force involved in this process is given by eq. (2.17) and is velocity dependent due to the Doppler shift. When the light source is spectrally narrow, as a laser is, this velocity dependence will take the atoms out of resonance as the beam slows down. This problem can be overcome by applying the Zeeman slower technique, first demonstrated by W. D. Phillips and H. J. Metcalf [2]. A Zeeman slower provides a position dependent Zeeman shift compensating the change in Doppler shift along the beam trajectory. This changing Zeeman shift is created by providing a magnetic field (see fig. 2.8) of the shape

$$B(z) = B_b + B_0\sqrt{1 - z/z_0} \tag{2.27}$$

with B_b the bias field, that does not change as a function of z and $z_0 = Mv_0^2/\eta\hbar k\Gamma$ the length of the device (most often referred to as a Zeeman slower). v_0 is the maximal initial velocity. η ($\eta < 1$) is a design parameter defined by $a = \eta a_{max}$ where a is the acceleration and $a_{max} = \hbar k\Gamma/2M$. The maximum magnetic field B_0 is given by $B_0 =$

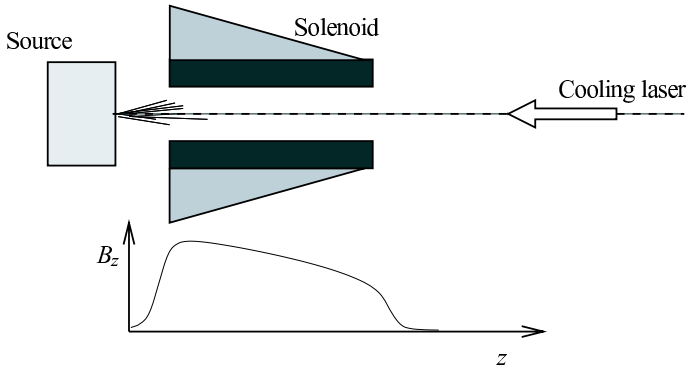

Figure 2.8: *Schematic lay-out of a Zeeman slower and its magnetic field shape.*

$\hbar k v_0/\mu_B$. Adding the Zeeman shift to the laser detuning and the Doppler shift in eq. (2.17), we can write for the force on the atoms in the Zeeman slower [52, 53]

$$\vec{F} = \hbar\vec{k}\frac{\Gamma}{2}\frac{s_0}{1+s_0+[2(\delta-\vec{v}\cdot\vec{k}+\mu' B(z)/\hbar)/\Gamma]^2} \tag{2.28}$$

Here, $\mu' = \mu_B(m_e g_e - m_g g_g)$, with g being the g-factor and m being the magnetic quantum number where the subscripts g and e refer to the ground and excited states.

2.5.2 The magneto optical trap

In order to create a trap for neutral atoms, the 1D optical molasses as discussed in section 2.3 can be extended to a 3D optical molasses consisting of three orthogonal pairs of counter propagating laser beams. Due to the strong friction force exerted on the atoms in the volume where the laser beams overlap, temperatures in the micro-Kelvin regime can be reached [54]. However, due to diffusion, atoms will drift out of the overlap volume, so there is no real spatial confinement. Spatial confinement can be obtained by adding an inhomogeneous magnetic field, as first demonstrated by E. L. Raab *et al.* [3] in 1987. This trapping scheme, called the Magneto Optical Trap (MOT), is nowadays used in many labs for a wide variety of applications.

In Fig. 2.9 the principle behind MOT operation is schematically depicted. Consider an atom having a $J_g = 0$ ground state and a $J_e = 1$ excited state. With no magnetic field applied, we define the transition frequency to be ω_0. We place our atoms in the field of two counter propagating laser beams, so when we tune the laser frequency ω_l just below ω_0 we are creating a 1D optical molasses. We recall that the $J_e = 1$ state has sub-states $m = 0, \pm 1$. The transitions $|J_g = 0, m_g = 0\rangle$ to $|J_e = 1, m_e = 0\rangle$, $|J_e = 1, m_e = -1\rangle$ and $|J_e = 1, m_e = 1\rangle$ are driven by π, σ^- and σ^+ polarized light respectively. We now

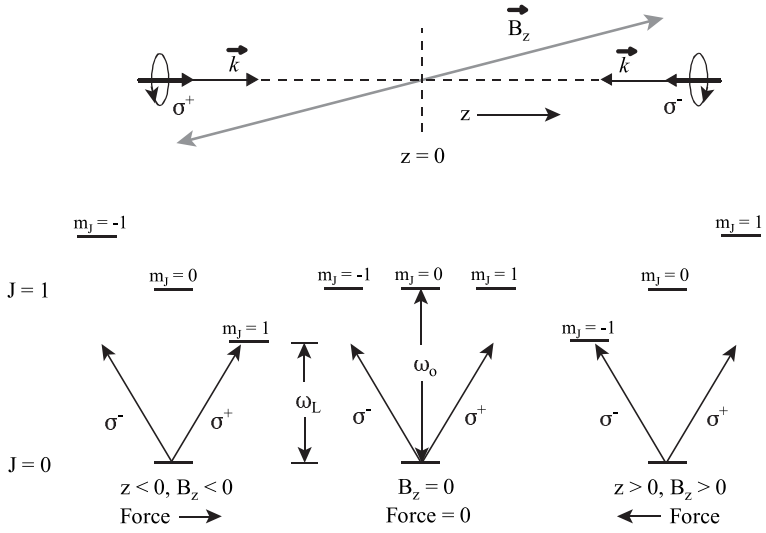

Figure 2.9: *Principles of MOT operation in one dimension.*

apply a magnetic field that is zero in the trap centre and increases linearly along the z-axis. Because of the Zeeman shift, the excited state with $m_e = +1$ is now shifted up for $B > 0$, whereas the state with $m_e = -1$ is shifted down.

For the example shown in Fig. 2.9 this implies that at positions $z > 0$ the magnetic field therefore tunes the $\Delta m = -1$ transition closer to resonance and the $\Delta m = +1$ further out of resonance. Consequently, the probability of absorbing light from the σ^- polarized laser beam is larger than the probability of absorbing light from the σ^+ polarized laser beam. If now the σ^- polarized laser beam comes from the right side, the atom will be pushed in the direction of the trap centre. For an atom at the other side of the trap centre, the process is the same, of course with the roles of $m_e = \pm 1$ and $\sigma^\pm$ interchanged. This scheme can be extended to three dimensions, using six instead of two laser beams. A linearly changing magnetic field with a zero-point in the trap centre can be obtained by two coils in anti-Helmholtz configuration, see fig. 2.10.

For optical molasses, the force on the atoms can be described as a damping coefficient times the velocity (Eq. 2.20). The quadrupole magnetic field together with the circularly polarized light add a position dependent term to this force:

$$F = -\beta v - \varkappa x \tag{2.29}$$

where $\varkappa$ is the spring constant, which in Doppler theory is defined as

$$\varkappa = \frac{\mu\prime}{\hbar k}\beta\frac{\partial B}{\partial x} \tag{2.30}$$

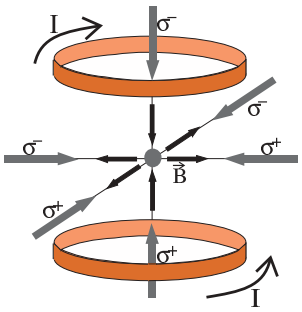

Figure 2.10: *Configuration of the MOT: anti-Helmholtz coils and circularly polarized beams.*

where $\partial B/\partial x$ is the magnetic field gradient. The velocity spread and the position spread are related by [40]

$$k_B T = \varkappa x_{rms}^2. \tag{2.31}$$

Here, k_B is the Boltzmann constant and T the temperature. x_{rms} is the rms value of the MOT cloud radius. If the trapping parameters are well known and Eq. 2.30 is valid, the temperature of the atoms in a MOT cloud can be obtained by just measuring the radius of the MOT cloud. For even isotopes of Sr Xu et al. [17] found that $\varkappa$ is well described by Doppler theory.

2.5.3 Trapping time in a MOT

The average time calcium atoms stay trapped in the MOT is limited by various loss mechanisms. The time evolution of the number of atoms N trapped in the MOT can be modelled by the differential equation [7]

$$\frac{dN}{dt} = R - \xi N - \chi \int n(r)^2 d^3 r, \tag{2.32}$$

where R is the atom capture rate, ξ is the linear loss rate coefficient, χ is the rate coefficient for two-body collisions, $n(r)$ is the atomic density and r the space variable. The linear loss from a calcium MOT consists of two processes: the loss due to a 'leak' in the level structure of calcium, and the loss due to collisions with the background gas in the MOT chamber.

Level structure loss

On average, after 10^5 $4s\ ^1S_0 - 4p\ ^1P_1$ cycles, the atom decays from the excited $4p\ ^1P_1$ state to the $3d\ ^1D_2$ state instead of the $4s^2\ ^1S_0$ ground state. From there, most atoms

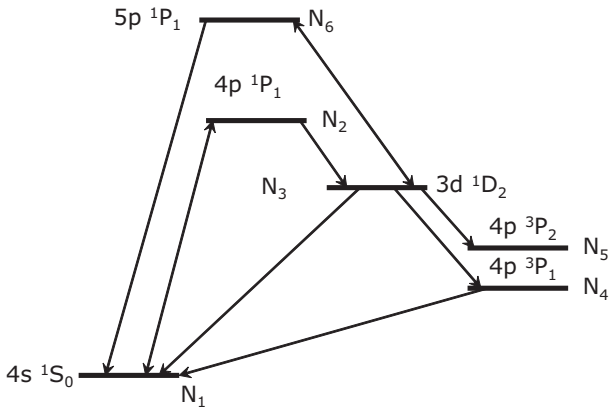

Figure 2.11: *An overview of the relevant levels of calcium in the MOT. See Table 2.4 for the relevant transition rates.*

end up, with some delay, in the $4s\ ^1S_0$ ground state again via the $4p\ ^3P_1$ state. However, about 24atoms decay from the $3d\ ^1D_2$ state to the long lived $4p\ ^3P_2$ state. Once atoms end up there, they will drift out of the trap before they decay back again to the ground state. This leak may be plugged by using a repump laser which pumps the atoms form the $^1D_2$ level to the $5p\ ^1P_1$ level from where the atoms can decay back into the ground state.

A rate equation analysis can be done to calculate the effect of the aforementioned loss mechanisms. The rate equation model is set up following Figure 2.11 and Table 2.4, in which the relevant levels and the transition rates between these levels (as calculated by Froese Fischer and Tachiev [55]) are given. Using those numbers, the following system of coupled differential equations can be constructed and solved:

$$\begin{aligned}
\dot{N}_1 &= R-(\Gamma_{12}+\xi+R_d)N_1+\Gamma_{21}N_2+\Gamma_{31}N_3+\Gamma_{41}N_4+\Gamma_{61}N_6\\
\dot{N}_2 &= \Gamma_{12}N_1-(\Gamma_{23}+\Gamma_{21}+\xi+R_d)N_2\\
\dot{N}_3 &= \Gamma_{23}N_2-(\xi+\Gamma_{31}+\Gamma_{34}+\Gamma_{35}+W+R_d)N_3+\Gamma_{63}N_6\\
\dot{N}_4 &= \Gamma_{34}N_3-(\Gamma_{41}+\xi+R_d)N_4\\
\dot{N}_5 &= \Gamma_{35}N_3-(\xi+R_d)N_5\\
\dot{N}_6 &= WN_3-(\Gamma_{63}+\Gamma_{61}+\xi+R_d)N_6. \qquad (2.33)
\end{aligned}$$

Here, R is the loading rate of the trap, W is the repumping rate and ξ is a parameter representing the trap losses due to collisions of trapped atoms with background gasses in the trap chamber, cf. Eq. 2.32. R_d is the drift rate, taking into account the losses due to the fact that atoms can simply drift out of the trap. This drift rate loss depends on the velocity and the size of the trapping region d_{tr}, and may be approximated by

i	j	Γ_{ij} [Hz]
1	2	$\frac{s_0\Gamma/2}{1+(2\delta/\Gamma)^2}$
2	1	2.19×10^8
3	1	40
4	1	4096
6	1	$2.7 \cdot 10^5$
2	3	3271
6	3	$1.2 \cdot 10^7$
3	4	380
3	5	134
3	6	W

Table 2.4: *Transition rates between levels i and j in calcium, see also Figure 2.11. The rates are taken from Ref. [55].*

$$R_d = \frac{v}{d_{tr}} \tag{2.34}$$

where v depends on the trap temperature T via $v = \sqrt{k_B T/M}$ with M the mass of the atom. These coupled differential equations were solved numerically using the Matlab ode45 solver.

In the experiment, the decay of the MOT fluorescence is measured as a function of time after switching off the loading of the MOT. In the calculation we therefore set $R = 0$. In a first calculation, the losses due to background collisions were also neglected, so ξ was set 0. To calculate the trapping time without repumping, W was set 0 as well. As an example, a typical value of 1 was taken for the fraction δ/Γ. The ratio I/I_s was varied between 0.1 and 1. The resulting numerical solution for $N_2(t)$ is fitted with an exponential decay as a function of time to obtain a trapping $(1/e)$ time. Here the population N_2 was chosen since this is the population that in the experiment is reflected in the measured MOT fluorescence. In Figure 2.12 the $1/e$ trapping time is given as function of the $s_0 = I/I_s$.

Background collision loss

Strictly speaking, ξ should have a non-zero value. According to ref. [20] and references therein, the value for ξ can be estimated using $\xi = P/(2.0 \times 10^{-8})$ with P the background pressure in the trapping chamber in mbar. In the AlCatraz experiment, the background pressure is typically within the 10^{-9} to 10^{-8} mbar range. Substituting $P = 5 \times 10^{-9}$ mbar seems therefore reasonable, resulting in $\xi = 0.25$. This however barely affects the trapping time, as changes are $< 10^{-3}$. Trapping time limitations arising from interactions with the background gas seem therefore very unlikely.

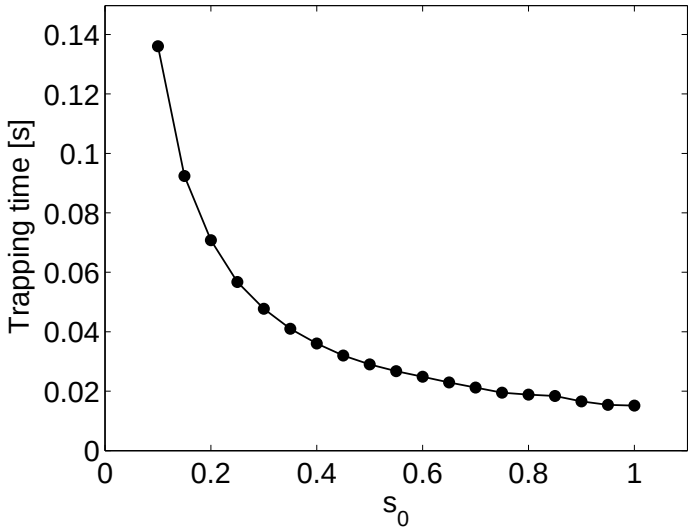

Figure 2.12: *Trapping times as function of the saturation fraction I/I_s taken from the solutions of Eq. (2.33).*

Ca-Ca collision loss

In Eq. (2.32) the relation is given that governs the time evolution of the number of atoms trapped in the MOT. If cold collisions become significant, we have to take into account the density distribution of the trapped atoms. One can distinguish between two trap volume and density regimes. In the lower density regime, the volume will stay constant and the density will increase if the number of trapped atoms increases. Above a certain critical density, the density will stay constant and the volume will increase [8, 56].

In the constant volume regime, the spatial distribution of atoms in the trap is Gaussian and we have for the time evolution of the atoms in the trap [8]:

$$\frac{dN}{dt} = R - \xi N - \chi \frac{N^2}{(\sqrt{2\pi}a)^3} \tag{2.35}$$

where N is the number of atoms and a is the waist of the atomic cloud which is related to temperature and trap parameters [40]. This differential equation can be analytically solved leaving χ as a direct fitting parameter to load and decay curves. Eq. (2.35) is a so called *Ricatti equation* and a solution reads [57]:

$$N(t) = \frac{2\zeta N_0 + (2R - N_0\xi)\tanh(\zeta t)}{2\zeta + \left(\xi + 2N_0 \frac{\chi}{(\sqrt{2\pi}a)^3}\right)\tanh(\zeta t)} \tag{2.36}$$

where ζ is defined as

$$\zeta = \frac{\sqrt{\xi^2 + 4R\frac{\chi}{(\sqrt{2\pi}a)^3}}}{2}. \tag{2.37}$$

Expressions for loading and decay of the trap can be given. In case of decay of the trap we have $N_0 \neq 0$ and $R = 0$ and eq. (2.36) can be simplified to

$$N_D(t) = \frac{N_0\xi}{(\xi + N_0\chi)\exp(\xi t) - N_0\chi} \tag{2.38}$$

yielding the well known and expected exponential decay expression $N_0\exp(-\xi t)$ if $\chi = 0$.

For loading the trap we have $N_0 = 0$ and $R \neq 0$. For these parameters Eq. (2.36) simplifies to

$$N_L(t) = \frac{R\tanh(\zeta t)}{2\zeta + \xi\tanh(\zeta t)}. \tag{2.39}$$

If the two-body collision rate $\chi = 0$ the expression for the number of atoms $N_L(t)$ becomes

$$N_L(t) = \frac{R}{\xi}[1 - \exp(-\xi t)]. \tag{2.40}$$

At low trap densities (in the case of alkaline-earth elements $< 10^{10}$ cm^{-3} or $< 10^7$ atoms, [8])[1] which are used in our experiments, the Ca-Ca collision losses can be neglected and both trap load and decay curves will be exponential.

The Ca-Ca collision contribution to the trap loss rate is further discussed in refs. [4,7,58], where the last two specifically deal with calcium. As mentioned above, in low densities used in our experiments it does not play a significant role in the trap dynamics of the MOT.

[1] It is pointed out that these limits are considerably higher than the ones for alkali elements, cf. [56].

2.5.4 Statistics of single or few atoms in a MOT

Poissonian distribution of atoms in the MOT

The trap population can be described by a simple linear loss model, where at equilibrium:

$$\frac{dN}{dt} = R - \frac{N}{\tau_{trap}} = 0 \tag{2.41}$$

where N is the number of particles in the trap, R is the trap loading rate and τ_{trap} is the life time of the trap. Trapping a low number of atoms in a MOT can be described as a Markov process: the probability of having a certain number of atoms in the trap at a certain time interval is entirely determined by the number of atoms in the previous time interval. A time Δt can be defined in which the number of atoms in the trap can be raised by one, can be lowered by one or can stay the same, according to the following transition probabilities p:

$$p(N \to N+1) = R\Delta t \tag{2.42}$$
$$p(N \to N-1) = \xi N \Delta t \tag{2.43}$$
$$p(N \to N) = 1-(R+\xi N)\Delta t \tag{2.44}$$

where $\xi = \tau_{trap}^{-1}$. The Chapman-Kolmogorov theorem [59] can now be applied: the probability to have N particles in the trap at a time $t+\Delta t$, $P(N, t+\Delta t)$, is written as the sum of terms, each of which represents the probability of a previous number of atoms ($N+1$, $N-1$ or N) multiplied by the probability of a transition to the number of atoms N:

$$P(N,t+\Delta t) = \\ = R\Delta t P(N-1,t) + \xi(N+1)\Delta t P(N+1,t) + (1-(R+\xi N)\Delta t)P(N,t). \tag{2.45}$$

From the quotient

$$\frac{P(N,t+\Delta t)-P(N,t)}{\Delta t}$$

and for $\Delta t \to 0$, we obtain:

$$\frac{\partial}{\partial t}P(N,t) = R\cdot P(N-1,t) + \xi(N+1)\cdot P(N+1,t) - (\xi N+R)\cdot P(N,t) \tag{2.46}$$

which is the so-called birth-death model presented by Ruschewitz *et al.* [60]. We are interested in the stationary solution of this differential equation. A stochastic process

$X(t)$ is stationary if $X(t)$ and the process $X(t+\epsilon)$ have the same statistics for any ϵ [59]. In this case, it means that $\frac{\partial}{\partial t}P(N,t)=0$. By substitution, it is easily shown that a solution is given by the Poisson distribution

$$P(N)=\frac{\langle N\rangle^N}{N!}e^{-\langle N\rangle}$$

for integer $N\geq 0$. The mean value $\langle N\rangle$ equals $R\tau_{trap}$, as follows from eq. 2.41.

Time correlation of single atom data

The model can also be used to determine the trap lifetime of single atoms in the trap, using time correlation analysis. The time correlation $\langle N(t+\tau),N(t)\rangle$ can be studied by the covariance

$$\langle N(t+\tau),N(t)\rangle=\langle N(t+\tau)N(t)\rangle-\langle N(t)\rangle^2 \tag{2.47}$$

which for $\tau=0$ is the variance

$$\sigma^2=\langle N^2\rangle-\langle N\rangle^2.$$

The time correlation function for stationary Markov processes is an exponential function of the time delay τ [59], and can be written as

$$G(\tau)=\sigma^2 e^{-\frac{\tau}{\tau_c}}, \tag{2.48}$$

where τ_c is the correlation time. The trap life time of calcium atoms in a MOT is interpreted as the correlation time, and the variance for Poissonian distributions is given by $\sigma^2=\langle N\rangle=R\tau_{trap}$. The time correlation $G(\tau)$ for calcium atoms in a MOT can therefore be given as

$$G(\tau)=R\tau_{trap}e^{-\frac{\tau}{\tau_{trap}}}. \tag{2.49}$$